Journal of Geoscience and Environment Protection, 2025, 13(4), 393-414
https://www.scirp.org/journal/gep
ISSN Online: 2327-4344
ISSN Print: 2327-4336

Comparative Analysis of Machine Learning Algorithms for Optimal Land Use and Land Cover Classification: Guiding Method Selection for Resource-Limited Settings in Tiaty, Baringo County, Kenya

John Kapoi Kipterer*, Mark K. Boitt, Charles N. Mundia

The Institute of Geomatics, GIS and Remote Sensing (IGGReS), Dedan Kimathi University of Technology, Nyeri, Kenya
Email: *karantili@gmail.com

How to cite this paper: Kipterer, J. K., Boitt, M. K., & Mundia, C. N. (2025). Comparative Analysis of Machine Learning Algorithms for Optimal Land Use and Land Cover Classification: Guiding Method Selection for Resource-Limited Settings in Tiaty, Baringo County, Kenya. *Journal of Geoscience and Environment Protection, 13,* 393-414.
https://doi.org/10.4236/gep.2025.134021

Received: March 23, 2025
Accepted: April 20, 2025
Published: April 23, 2025

Abstract

Arid and semiarid regions face challenges such as bushland encroachment and agricultural expansion, especially in Tiaty, Baringo, Kenya. These issues create mixed opportunities for pastoral and agro-pastoral livelihoods. Machine learning methods for land use and land cover (LULC) classification are vital for monitoring environmental changes. Remote sensing advancements increase the potential for classifying land cover, which requires assessing algorithm accuracy and efficiency for fragile environments. This research identifies the best algorithms for LULC monitoring and developing adaptive methods for sensitive ecosystems. Landsat-9 imagery from January to April 2023 facilitated land use class identification. Preprocessing in the Google Earth Engine applied spectral indices such as the NDVI, NDWI, BSI, and NDBI. Supervised classification uses random forest (RF), support vector machine (SVM), classification and regression trees (CARTs), gradient boosting trees (GBTs), and naïve Bayes. An accuracy assessment was used to determine the optimal classifiers for future land use analyses. The evaluation revealed that the RF model achieved 84.4% accuracy with a 0.85 weighted F1 score, indicating its effectiveness for complex LULC data. In contrast, the GBT and CART methods yielded moderate F1 scores (0.77 and 0.68), indicating the presence of overclassification and class imbalance issues. The SVM and naïve Bayes methods were less accurate, rendering them unsuitable for LULC tasks. RF is optimal for monitoring and planning land use in dynamic arid areas. Future research should explore hybrid methods and diversify training sites to improve performance.

Keywords

Support Vector Machine, Random Forest, Classification and Regression Trees. Gradient Boosting Trees, Naïve Bayes, Semiarid, Weighted F-1 Score, Land Use and Land Cover

1. Introduction

Land use and land cover (LULC) classification is crucial in environmental monitoring and resource management, especially in dynamic and fragile ecosystems (Fang et al., 2022). Accurate LULC mapping is a foundation for understanding land dynamics, monitoring environmental changes, and informing sustainable policy and land management practices (Abebe et al., 2022). With the advent of remote sensing technologies combined with machine learning algorithms, the field of LULC classification has undergone a significant transformation, addressing the limitations of traditional manual and statistical methods (Wang et al., 2022). These advancements offer improved accuracy, scalability, and efficiency, particularly valuable in arid and semiarid regions where rapid landscape transformations, such as bushland encroachment and crop cultivation, are prevalent (Tamayo-Vera et al., 2024). This study addresses a critical gap in the literature by comprehensively evaluating the performance of multiple machine learning algorithms for LULC classification in Kenya's arid and semi-arid lands (ASALs), a region characterized by unique environmental challenges and limited prior research on this specific topic.

Integrating remote sensing data with machine learning (ML) techniques has become increasingly prominent globally. Algorithms such as random forest (RF), support vector machines (SVMs), classification and regression trees (CARTs), tree boosting (GBT) machines, and naïve Bayes, among others, have demonstrated high accuracy and adaptability in diverse environmental conditions (Avci et al., 2023; Chowdhury, 2024). The development of computational platforms such as the Google Earth Engine (GEE) has further enhanced these methods' capabilities (Amani et al., 2020). Owing to its cloud-based processing capabilities and access to extensive satellite datasets such as Landsat and Sentinel imagery, GEE enables real-time, large-scale analysis of land cover changes (Ghosh et al., 2022). This integration facilitates efficient monitoring of critical transformations, including urban expansion, deforestation, agricultural intensification, and climate-driven ecosystem shifts (Cao et al., 2022).

Supervised machine learning algorithms, which are widely applied across various domains, excel at addressing high-dimensional problems where traditional statistical methods fall short (Maini & Govinda, 2017; Talukdar et al., 2020). These algorithms are particularly effective in LULC classification because they can capture complex, nonlinear relationships between land features and satellite imagery data. Evaluating algorithms such as random forest, support vector machines, and regression trees in arid and semiarid environments is essential for accurate LULC

assessment (Adugna et al., 2022). For example, CART operates as an individual decision tree classifier that splits data at each node on the basis of normalised information gain. The SVM uses kernel functions to project data into a multidimensional space, maximising class separation (Praticò et al., 2021). Tree boosting (GBT), which integrates multiple decision trees, enhances model accuracy and has proven effective in remote sensing image classification (Chen et al., 2017). Moreover, naïve Bayes, though simple to implement, assumes feature independence, a limitation in complex remote sensing datasets (Firthouse Mohammed Yashin et al., 2020).

Kenya, where more than 80% of the land comprises arid and semiarid lands (ASALs), faces unique challenges, such as climate variability, population growth, and agricultural expansion, which significantly alter land use patterns (Amwata & Nyariki, 2021). In these regions, bushland encroachment and declining agricultural productivity threaten traditional pastoral and agro-pastoral livelihoods. Accurate LULC classification is crucial for monitoring vegetation dynamics, assessing land degradation, and designing adaptive land management strategies (Badapalli et al., 2025).

The Tiaty region of Baringo County, situated within Kenya's ASAL zone, has experienced significant LULC changes over the past three decades (Greiner et al., 2021a). Bushland encroachment and (Bollig et al., 2014) increasing crop cultivation have notably transformed the landscape, mirroring the trends observed in neighboring regions such as Ethiopia (Fentaw & Abegaz, 2024). These transformations threaten biodiversity, disrupt traditional land use systems, and impact agricultural productivity, necessitating an urgent assessment of machine learning algorithms to classify these changes accurately (Bogale et al., 2022). Understanding these transformations' spatial and temporal dynamics is essential for developing strategies to mitigate their impact on pastoral and agro-pastoral livelihoods (Fentaw & Abegaz, 2024).

Remote sensing technologies and machine learning algorithms have demonstrated potential for accurate LULC classification globally, their application in Kenya's ASALs remains limited and often lacks comprehensive evaluations of multiple algorithms. The lack of a robust, scalable, and accurate LULC mapping framework for this fragile ecosystem hinders effective land resource monitoring and management. This study addresses this critical gap by assessing the performance of five machine learning algorithms using Landsat 9OLI/TIRS imagery on GEE, aiming to enhance resource monitoring and inform sustainable land management strategies.

Previous research has often relied on single classification techniques, neglecting a comprehensive comparison of alternative machine learning models. For example, maximum likelihood classification (MLC) has been widely applied in this region, as referenced in (Amboka & Ngigi, 2015; Kiage & Douglas, 2020; Kimtai et al., 2024; Ochuka et al., 2019). These studies focused on phenomena such as Prosopis proliferation, human-induced changes, and water level variations in Rift Valley lakes and the Baringo region. Moreover, random forest algorithms have been used to assess the spatiotemporal dynamics of LULC, with a particular focus

on the impact of Prosopis invasion in East Pokot (Kumar Basukala et al., 2019; Mbaabu et al., 2019). This underscores the need for a more comprehensive evaluation of multiple algorithms to improve the accuracy, efficiency, and scalability of LULC studies in this context.

This study evaluated five machine learning algorithms random forest (RF), support vector machine (SVM), classification and regression trees (CARTs), gradient boosting trees (GBTs), and naïve Bayes for classifying land use and land cover (LULC) in Tiaty, Baringo County. By utilizing Landsat 9 satellite imagery processed on the Google Earth Engine (GEE), the accuracy, efficiency, and scalability of each algorithm are assessed. The objective is to identify the most effective algorithm for LULC mapping in arid and semiarid regions, which will aid in resource monitoring and guide researchers and practitioners in selecting the most suitable machine learning classifiers for these dynamic environments.

The study hypothesizes that the random forest (RF) algorithm, when combined with remote sensing data and processed on GEE, will outperform other machine learning methods in accurately and efficiently classifying land use and land cover in Tiaty, Baringo County. These findings will contribute to a better understanding of robust machine learning methods suitable for LULC classification in dynamic arid and semiarid lands (ASALs) and provide practical guidance for selecting optimal machine learning methods for rapid implementation in similar analyses.

2. Materials and Methods

2.1. Description of the Study Area

Tiaty is a region in Baringo County, which is part of the Rift Valley Province of Kenya (refer to **Figure 1**). It is situated on the floor of the rift valley, with an average altitude of 1000 m above sea level. It lies between latitudes 00˚13' S and 1˚40' N and longitudes 35˚36' E and 36˚30' E.

The climate is classified as semiarid, with temperate to warm temperatures, and is prone to recurrence. The region experiences a semiarid climate characterized by moderate to warm temperatures and a high likelihood of periodic droughts (Greiner et al., 2021a). This climate classification is reflected in the dominant vegetation of the acacia bush savannah, which is well adapted to thrive in arid conditions (Greiner et al., 2021b; Vehrs, 2016).

The rugged topography, consisting of lowland plains, rolling hills, and mountain ranges, further influences local climate patterns (Greiner et al., 2021b). These physical features can create variations in temperature, precipitation, and wind patterns across a region. The average temperature ranges from 25˚C to 30˚C, with occasional highs exceeding 35˚C and a mean annual rainfall ranging from 450 - 900 mm (Kapoi & Charles, 2015). The average temperature ranges from 25˚C to 30˚C, with occasional highs exceeding 35˚C, and a mean annual rainfall ranging from 450 - 900 mm (Kapoi & Charles, 2015). The dominant vegetation is open Acacia/Combretum wooded grassland, supporting primarily livestock production through specialized pastoralism for the past two centuries (Bollig & Österle, 2013).

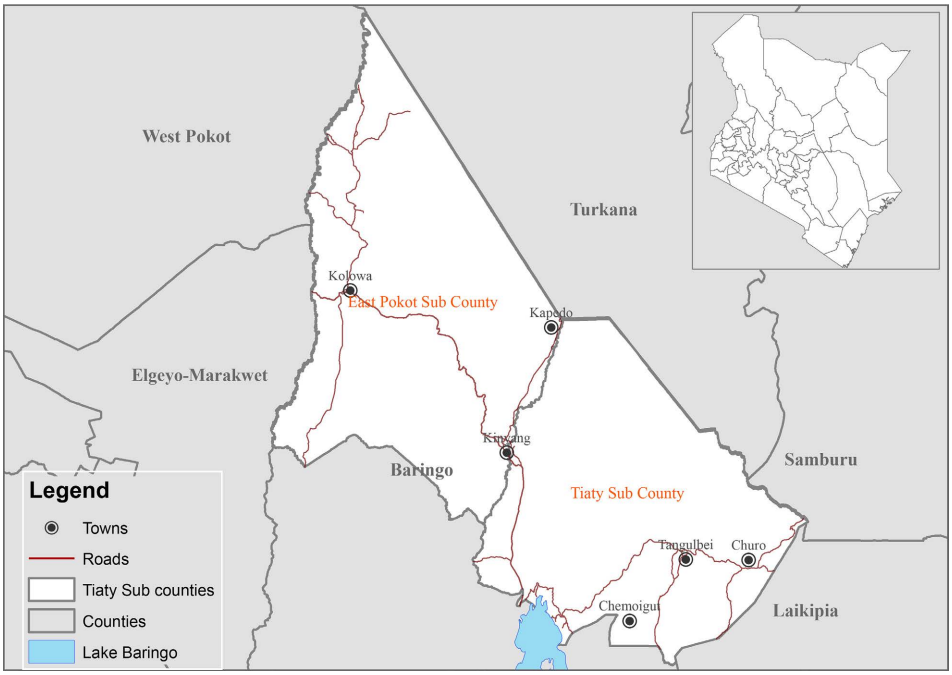

Figure 1. Map of Tiaty subcounties.

2.2. Data Sources

The research utilized Landsat-9 Operational Land Imager (OLI) and Thermal Infrared (TIRS) data with a 30 m resolution (Earth Resources Observation and Science (EROS) Center, 2020). The data, encompassing all spectral bands, were acquired during the agronomic period of January to April 2023. The potential impact of seasonal variations on spectral signatures will be considered in the analysis. Additional auxiliary boundary GIS data for Tiaty in Baringo County were acquired from RCMRD, Kenya, to ensure accurate spatial referencing and classification within the study area boundaries.

3. Methodology Workflow

3.1. Data Processing

The Landsat-9 images were processed via Google Earth Engine applications, where the cloud mask method removed pixels affected by clouds. To ensure that classifications were performed within the appropriate limits, the images were clipped to the boundaries of the study area. Spectral indices, as outlined in the workflow in Figure 2, with detailed formulas provided in Table 1, were employed for classification purposes.

Cloud masking in the Google Earth Engine (GEE) was employed to identify and eliminate pixels contaminated by clouds in satellite imagery, thereby enhancing the quality and reliability of the analyses. GEE's built-in cloud masking function was used, employing bitwise operations to identify and mask cloudy pixels. The clip function (.clip ()) in GEE was implemented to confine the satellite imagery dataset to the area of interest (AOI) corresponding to the user-defined geometry

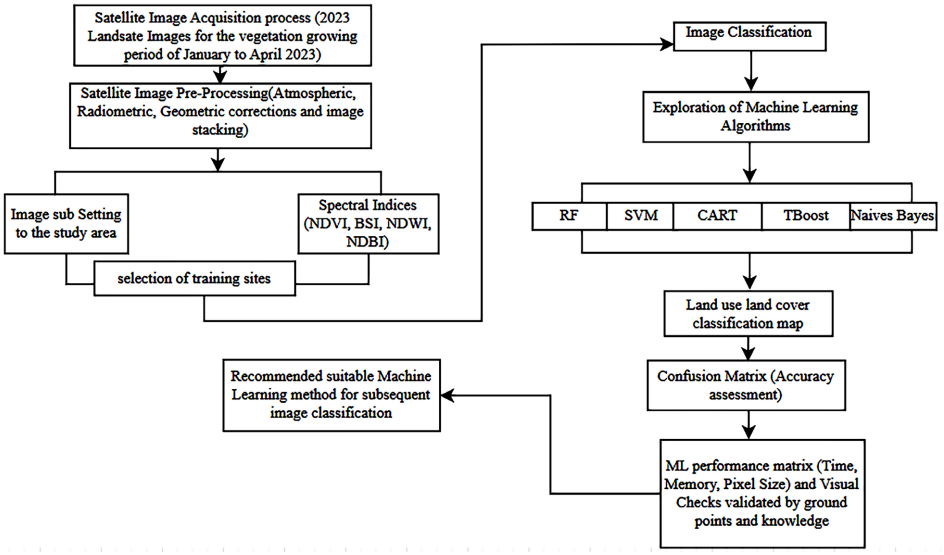

Figure 2. Methodology workflow.

Table 1. Spectral indices.

Indices	Formula
Normalized difference Vegetation Index (NDVI)	$NDWI = (NIR - RED)/(NIR + Red)$ (Li et al., 2021)
Normalized Difference Water Index (NDWI)	$NDWI = (NIR - SWIR)/(NIR + SWIR)$ (Zha et al., 2003)
Bare Soil index (BSI)	$BSI = ((Red + SWIR) - (Nir + Blue))/((Red + SWIR) + (Nir + Blue))$ (Rikimaru et al., 2002)
Normalized Difference Building Index (NDBI)	$NDBI = (SWIR - NIR)/(SWIR + NIR)$ (Zha et al., 2003)

of Tiaty, the study area. This focused the analysis on the boundaries of the study area, resulting in reduced computational requirements. The effective integration of cloud masking and clipping is crucial for generating high-quality data for analysis.

The normalized difference vegetation index (NDVI) was used to differentiate between dense shrubland and dryland forests. The normalized difference water index (*NDWI*) was used to distinguish between water bodies and wetlands, whereas the bare soil index (*BSI*) was used to identify bare surfaces. The normalized difference built-up index (*NDBI*) was also applied to identify urban built-up areas. These indices were selected based on their established effectiveness in differentiating between various land cover types in arid and semi-arid environments.

3.2. Land Use/Land Cover Classification

The overall accuracy is the number of correctly classified pixels divided by the total number of validation pixels, as shown in Equation (1) (Elmahdy & Mohamed, 2023; Pham et al., 2023).

$$OA = \frac{\sum_{i=1}^{k} n_{ii}}{N} \quad (1)$$

where:

n_{ii} is the number of correctly classified pixels for class *i*.

N is the total number of validation pixels.

The kappa coefficient is a measure of the agreement between the classification map and the reference data, considering the agreement that might be expected by chance, as shown in Equation (2):

$$\text{Kappa} = \left(p_o - p_e\right) / \left(1 - p_e\right) \quad (2)$$

where p_o is the probability of observed agreement and where p_e is the probability of chance agreement.

3.3. Performance Metrics

i) F-1 score

The harmonic means of precision and recall, the F-1 score, are used to evaluate machine learning and information retrieval. An imbalance between positive and negative categories makes model performance evaluation more balanced (Pham et al., 2023). The F-1 score is the harmonic mean of precision and recall, or the ratio of genuine positives to true and false positives, which can be evaluated via Equations (3)-(5):

The F1 score is shown in Equation (3):

$$F1 = 2 \cdot \frac{\text{Precision} \cdot \text{Recall}}{\text{Precision} + \text{Recall}} \quad (3)$$

where:

$$\text{Precision} = \frac{TP}{TP + FP} \quad (4)$$

$$\text{Recall} = \frac{TP}{TP + FN} \quad (5)$$

where TP = true positives, FP = false positives and FN = false negatives.

ii) Weighted F-1 score

Although F-1 ratings are significant, the weighted F1 score serves to assess the model's performance across all categories (Hinojosa Lee et al., 2024). Weights tailored to problem specifications provide a more focused and refined assessment of model performance (Pham et al., 2023). The weights can be modified according to the specific demands of the task, facilitating a more precise and nuanced assessment of the model's performance (Lipton et al., 2014; Mayer et al., 2021; Pham et al., 2023). In these instances, the weighted F1 score more effectively evaluates the model's performance by incorporating the priority of precision and recall (Lipton et al., 2014). The weighted F-1 can be evaluated via Equation (6).

$$\text{Weighted F1-score} = \sum_{i=1}^{N} \left(\frac{\text{Support}_i}{\text{Total Support}} \right) \times \text{F1-score}_i \quad (6)$$

where:

N = Total number of classes, Support i = Number of true instances for the i-th class. Total Support = Sum of all support values. F1-score$_i$ = F1 score for the i-th class.

iii) Execution run-time

The execution duration of machine learning algorithms in the Google Earth Engine (GEE) is directly affected by several pivotal factors, including dataset size, algorithm complexity, available bandwidth for data transfer, and memory utilization, all of which are crucial in ascertaining the computational time necessary for performing machine learning tasks on GEE (Zhao et al., 2024). Understanding and improving these components will result in more effective and successful outputs and execution times (Farda, 2017).

3.4. Land Use/Land Cover Classification

Pixel-based supervised classification in the Google Earth Engine utilizes several classifiers within the Google Earth Engine. The classifiers include random forest (RF), support vector machine (SVM), classification and regression trees (CARTs), tree boosting (GBT), and naïve Bayes. Based on the knowledge of the study area, predominantly pastoral and agro-pastoral livelihood, a set of defined land use and land cover classes was determined, and a description of each class provided, as shown in Table 2, was established. Training sites were established for the classification process.

Table 2. Land use/Land cover classes.

Land use/cover classes	Description of the classes
Dryland Forest	The dryland forest, predominantly in mountainous reserved areas with dense tree vegetation
Water bodies	Any visible open water bodies such as lakes, rivers, water pans
Cropland	This is cultivated fields or farms
Grassland	Is the grass pasture of all species
Dense shrubland	Densely woody shrubs characterized by dense bushes
Sparse/open shrubland	Open bushes patched with open spaces
Built-up/Settlement	Built-up, settlements/schools characterized by buildings
Others	Shadows, clouds, bare soil, bare rock areas, and any other unidentified categories

4. Results

4.1. Land Use/Land Cover

Figure 3(a) illustrates a land use and land cover classification employing the support vector machine technique. The product inadequately classified the category labelled "Others", which includes shadows, clouds, bare soil, bare rock sections, and any other ambiguous classifications. Furthermore, there is inadequate classi-

fication of cropland, built-up areas, and grassland.

Figure 3(b) illustrates a land use and land cover classification using the Naïve Bayes machine technique. This method misclassifies and generalizes all the classes.

Figure 3(c) illustrates a land use and land cover classification using the Gradient Boost machine technique. The product has overclassified grassland in the southern part of the region.

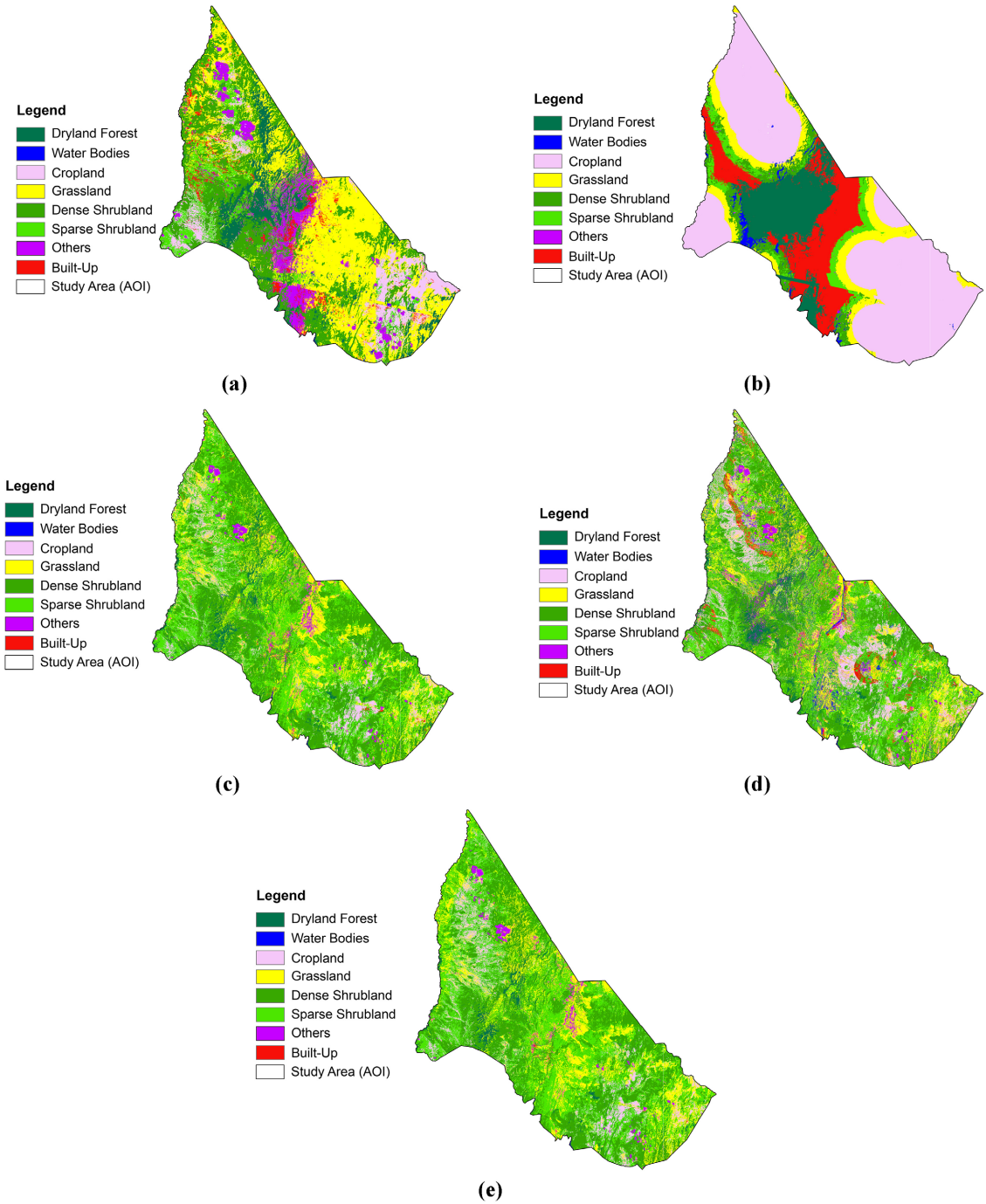

Figure 3. (a) Support vector machine; (b) Naïve Bayes; (c) Gradient tree boost; (d) Classification and regression tree; (e) Random forest.

Figure 3(d) illustrates a land use and land cover classification using the Classification and Regression Tree technique. The product excessively classified water bodies and built-up areas, resulting in speckle noise with circular patterns shape.

Figure 3(e) shows a classification of land use and land cover using the Random Forest methodology. The product provides the enhanced classification of land use/cover categories; however, an imbalanced classification in cropland cover has been noted in the northwestern part of the study area.

4.2. Accuracy Assessment

i) Evaluation of Accuracy and Runtime Performance Metrics

Table 3 presents the detailed accuracies and run times of the algorithms used, where the random forest method demonstrated an overall accuracy of 84.4% and a kappa of 81.7%, with a runtime of 2.757 seconds. The gradient tree boost (BGT) achieved an accuracy of 76.9% and a kappa of 73.1%; however, it had a slightly longer runtime of 2.91 seconds. The classification and regression tree (CART) technique exhibited moderate efficacy, achieving 68.8% accuracy and a kappa of 63.5%, while requiring a duration of 2.999 s, implying a trade-off between precision and computational expense.

Table 3. Accuracies and runtime.

Variable	SVM	RF	Tree Boost (BGT)	Naïve Bayes	CART
Overall Accuracy	0.3625	0.8438	0.76875	0.2875	0.6875
Kappa	0.2533	0.8173	0.73077	0.1712	0.6374
Pixels (N)	4,937,128.0000	4,937,128.0000	4,937,128.00000	4,937,128.0000	4,937,128.0000
Bands	19.0000	19.0000	19.00000	19.0000	19.0000
Memory (MB)	357.8400	357.8400	357.84000	357.8400	357.8400
Time(s)	3.8680	2.7570	2.91000	2.7580	2.9990

In contrast, the SVM achieved an accuracy of only 36.25%, a kappa statistic of 25.33%, and recorded the most extended runtime of 3.868 seconds, making it the least efficient option. In contrast, naïve Bayes displayed the lowest accuracy at 28.75%, a kappa of 17.12, and a duration of 2.758 seconds, indicating reduced predictive capability and limited efficiency.

The random forest is the most suitable algorithm for this study based on accuracy, reliability, and computational efficiency. Gradient boosting trees (GBT) provides a viable alternative, while CART balances accuracy and interpretability. SVM and naïve Bayes exhibited poor performance and are not recommended for this type of analysis.

ii) Performance Metrics for Accuracy Assessment and F-1 scores, including the Weighted F-1

a. Naïve Bayes (NB)

The naïve Bayes model results in Table 4 yield a producer accuracy (PA) of 3.45% and a user accuracy (UA) of 11.11%, with a low F1 score of 0.05, indicating difficulties in accurately classifying cropland. Dense shrubland achieved a PA of 17.39% and a UA of 40.00%, whereas Dryland Forest had a PA of 72.73% but a UA of only 17.39%, indicating confusion with other land types. Sparse shrubland had a PA of 5.56% and a UA of 20.00%, and built-up/settle land had a PA of 22.73% and a UA of 20.00%, resulting in a low F1 score of 0.21, highlighting issues in identifying built-up areas.

Table 4. Naïve bayes accuracies and F scores.

Num	Classes	PA (%)	UA (%)	Support (Ground Truth points)	F-1 Score	Weighted_ Average F1 Score
1	Dry Land Forest	0.72730	0.17391	11	0.28069982	0.019298113
2	Water Bodies	0.28571	0.40000	7	0.33333042	0.014583206
3	Grassland	0.78130	0.41670	32	0.54351871	0.108703743
4	Cropland	0.03448	0.11110	29	0.05262712	0.009538665
5	Dense Shrubland	0.17390	0.40000	23	0.24241157	0.034846663
6	Sparse Shrubland	0.05556	0.20000	18	0.08696197	0.009783221
7	Others	0.00000	0.00000	18	0.00000000	0.000000000
8	Built-up	0.22730	0.20000	22	0.21277791	0.029256962
				160		0.226010573

The weighted average F1 score of 0.23 highlights the model's poor classification performance, indicating significant misclassification across all classes. This low score reflects the model's struggle to balance precision and recall, leading to unreliable outputs. Thus, the naïve Bayes model is inadequate for land use classification in complex landscapes, limiting its use for environmental monitoring and land-use planning.

b. Gradient Tree Boost

The gradient boost model results in Table 5 for cropland yield a producer accuracy (PA) of 65.52% and a user accuracy (UA) of 73.08%, leading to an F1 score of 0.69. This indicates a significant performance improvement over the naïve Bayes model. Dense shrubland achieved a PA of 65.23% and a UA of 83.33%, and Dryland Forest had a PA of 90.91% and a UA of 62.50%, demonstrating better generalizability across land types. Sparse shrubland and built-up/settlement classes also improved markedly. Sparse shrubland had a PA of 88.89% and a UA of 69.57%, whereas built-up/settle land had a PA of 68.18% and a UA of 100.00%, resulting in a strong F1 score of 0.81. These results show that the model effectively captures distinct land cover categories.

Table 5. Gradient tree boost accuracies and F scores.

Num	Classes	PA (%)	UA (%)	Support (Ground Truth points)	F-1 Score	Weighted_ Average F1 Score
1	Dry Land Forest	0.9091	0.6250	11	0.7407438	0.05092613
2	Water Bodies	0.7143	1.0000	7	0.8333431	0.03645876
3	Grassland	0.8750	0.8485	32	0.8615463	0.17230925
4	Cropland	0.6552	0.7308	29	0.6909382	0.12523255
5	Dense Shrubland	0.6523	0.8333	23	0.7317738	0.10519249
6	Sparse Shrubland	0.8889	0.6957	18	0.7805222	0.08780875
7	Others	0.8333	0.6250	18	0.7142735	0.08035577
8	Built-up	0.6818	1.0000	22	0.8107980	0.11148472
				160		0.76976841

The weighted average F1 score of 0.77 indicates strong classification performance, indicating balanced precision and recall across classes. A higher weighted F1 score suggests that gradient boosting effectively reduces misclassification, making it a more reliable model for land use classification and suitable for environmental monitoring and planning.

c. Support Vector Machine (SVM)

The support vector machine (SVM) model results in Table 6 indicate a producer's accuracy (PA) of 37.93% and a user's accuracy (UA) of 23.91% for cropland, yielding a low F1 score of 0.29, reflecting misclassification issues. Dense shrubland achieved a PA of 47.83% and a UA of 33.33%, whereas Dryland Forest had a PA of 81.89% but a UA of only 50.00%, indicating confusion with other land types.

Table 6. Support vector machine accuracies and F scores.

Num	Classes	PA (%)	UA (%)	Support (Ground Truth points)	F-1 Score	Weighted_ Average F1 Score
1	Dry Land Forest	0.81890	0.5000	11	0.62089620	0.042686614
2	Water Bodies	0.28570	1.0000	7	0.44442716	0.019443688
3	Grassland	0.46875	0.6818	32	0.55554952	0.111109904
4	Cropland	0.37930	0.2391	29	0.29330734	0.053161956
5	Dense Shrubland	0.47830	0.3333	23	0.39284719	0.056471784
6	Sparse Shrubland	0.05560	0.0589	18	0.05720245	0.006435275
7	Others	0.22220	0.2857	18	0.24998047	0.028122803
8	Built-up	0.22720	0.6250	22	0.33325510	0.045822577
				160		0.363254600

Sparse shrubland and built-up/settle land also performed poorly, with sparse shrubland at PA 5.56% and UA 5.89% and built-up/settle land at PA 22.72% and UA 62.50%, resulting in a low F1 score of 0.33. These results suggest that the SVM model struggles to distinguish similar land cover classes, hindering its effectiveness in complex landscapes.

The weighted average F1 score of 0.36 shows challenges in classification accuracy. This low score highlights inconsistencies in precision and recall across land use classes, making SVM unreliable for land use classification. Therefore, SVMs may not be suitable for environmental monitoring and land-use planning, as they lack balanced classification across diverse land cover types.

d. CART

The CART model results in Table 7 for cropland yield a producer accuracy (PA) of 44.83% and a user accuracy (UA) of 65.00%, resulting in an F1 score of 0.53. This suggests moderate performance, indicating challenges in distinguishing cropland from other land covers. Dense shrubland achieved a PA of 60.87% and a UA of 66.67%, whereas Dryland Forest recorded a PA of 90.91% and a UA of 62.50%, reflecting superior classification. Sparse shrubland and built-up/settlement classes presented sparse shrubland with a PA of 66.67% and a UA of 70.59%, whereas built-up/settlement had a PA of 63.64% and a UA of 77.78%, culminating in a robust F1 score of 0.70. These results imply that the CART model facilitates improved classification of land cover types.

Table 7. CART accuracies and F scores.

Num	Classes	PA (%)	UA (%)	Support (Ground Truth points)	F-1 Score	Weighted_ Average F1 Score
1	Dry Land Forest	0.9091	0.6250	11	0.7407438	0.05092613
2	Water Bodies	0.7143	0.6250	7	0.6666729	0.02916694
3	Grassland	0.8434	0.8182	32	0.8306089	0.16612178
4	Cropland	0.4483	0.6500	29	0.5306292	0.09617653
5	Dense Shrubland	0.6087	0.6667	23	0.6363812	0.09147980
6	Sparse Shrubland	0.6667	0.7059	18	0.6857402	0.07714578
7	Others	0.8333	0.5556	18	0.6666880	0.07500240
8	Built-up	0.6364	0.7778	22	0.7000310	0.09625426
				160		0.68227362

The weighted average F1 score of 0.68 suggests that CART offers enhanced precision and recall across various classes, rendering it a more dependable option for environmental monitoring and land-use planning. However, some misclassification issues remain, particularly in differentiating cropland from shrubland.

e. Rand Forest (RF)

The results for the random forest model in Table 8 regarding Cropland indicate a producer's accuracy (PA) of 86.21% and a user's accuracy (UA) of 78.13%, culminating in a high F1 score of 0.82. This reflects strong classification performance, with minimal misclassification errors. Dense shrubland achieved a PA of 86.61% and a UA of 79.17%. In contrast, Dryland Forest had a PA of 90.91% and a UA of 71.43%, underscoring the model's capacity to distinguish between different land cover types accurately.

Table 8. RF accuracies and F scores.

Num	Classes	PA (%)	UA (%)	Support (Ground Truth points)	F-1 Score	Weighted_ Average F1 Score
1	Dry Land Forest	0.9091	0.7143	11	0.8000125	0.05500086
2	Water Bodies	0.7143	1.0000	7	0.8333431	0.03645876
3	Grassland	0.8750	0.9032	32	0.8888764	0.17777528
4	Cropland	0.8621	0.7813	29	0.8197137	0.14857310
5	Dense Shrubland	0.8661	0.7917	23	0.8272305	0.11891439
6	Sparse Shrubland	0.9444	0.8947	18	0.9188785	0.10337383
7	Others	0.7778	0.8235	18	0.7999979	0.08999976
8	Built-up	0.7727	0.9444	22	0.8499655	0.11687026
	Total			160		0.84696623

The sparse shrubland and built-up/settlement classes also demonstrated commendable performance. Sparse shrubland had a PA of 94.44% and a UA of 89.47%, whereas built-up/settle land had a PA of 77.27% and a UA of 94.44%, resulting in a high F1 score of 0.85. Tables 4-8 provide a detailed breakdown of the performance metrics for each algorithm, including producer's accuracy, user's accuracy, F1-scores for individual land cover classes, and the weighted average F1-score. These results further support the conclusions drawn from the overall accuracy and kappa statistics.

5. Discussions

5.1. Land Cover Classification Maps

Land use and land cover (LULC) classification is essential in remote sensing and influences urban planning, agriculture, and ecosystem management. This discussion evaluates five machine learning techniques: SVM, naïve Bayes, gradient tree boost, CART, and random forest for LULC classification, as shown in Figures 3(a)-(e). While SVM manages high-dimensional data and establishes solid classification boundaries, it struggles with complex land cover types, such as shadows and clouds and classes with high variability, such as cropland and grassland (Figure 3(a)). These limitations are likely due to the algorithm's sensitivity to param-

eter settings and the need for careful feature selection and optimization.

Naïve Bayes struggles due to its feature independence assumption, often violated in remote sensing data with correlated spectral bands and spatial features (**Figure 3(b)**). This inherent limitation renders it unsuitable for complex LULC tasks, particularly those involving high-dimensional datasets. The gradient tree boost can handle nonlinear relationships and improve accuracy through ensemble learning; this has been observed in previous studies (Pham et al., 2023). In this study, these methods tend to overclassify dominant classes such as grasslands, likely due to class imbalance or overfitting (**Figure 3(c)**). This highlights the importance of addressing class imbalance and employing regularization techniques to prevent model bias. Similarly, CART shows overclassification of water bodies and built-up areas, causing speckle noise and circular patterns, possibly due to overly complex decision boundaries (**Figure 3(d)**). These results suggest that parameter optimization, such as pruning, is crucial for improving CART's performance in heterogeneous landscapes.

The random forest model is the most effective of the five methods; it uses ensemble learning and feature randomness to manage LULC data complexity and improve classification accuracy (**Figure 3(e)**). However, it shows imbalanced cropland classification in the northwestern area, likely due to insufficient training samples or challenges in capturing spectral variability; previous research identified a similar scenario while classifying in the Sahel region of West Africa [48]. Despite this limitation, the random forest model demonstrates robust performance for LULC classification, provided that sufficient and representative training data are used. This study underscores the necessity of suitable machine-learning techniques for LULC classification and highlights the significance of hybrid approaches and enhanced feature extraction across diverse landscapes.

5.2. Evaluation of Accuracy and Runtime Performance Metrics

The performance metrics of the five machine learning algorithms for land cover classification emphasize their accuracy, kappa statistics, and efficiency. The random forest method stands out as the top performer, achieving 84.4% accuracy and 81.7% kappa, while running for 2.757 seconds. This highlights its effectiveness in managing complex data efficiently. However, the accuracy achieved in this study could be further improved through the exploration of more advanced techniques. Studies in Ethiopia (Fentaw & Abegaz, 2024) have reported accuracies approaching 90% using hybrid random forest-CNN models with Sentinel-2 data, suggesting that hybrid approaches could enhance the accuracy of LULC mapping. Furthermore, research in Saudi Arabia (Sun & Ongsomwang, 2023) has shown the advantages of deep learning (U-Net) over random forests for edge detection in arid regions, indicating the potential for further improvements.

The gradient tree boost is a strong alternative with 76.9% accuracy and 73.1% kappa, though it has a longer runtime of 2.91 seconds. Despite its competitive accuracy, its high computational cost limits its suitability for large-scale use. The

classification and regression tree (CART) achieves 68.8% accuracy and 63.5% kappa with a runtime of 2.999 seconds. While less accurate, CART is suitable when interpretability is prioritized over precision. Machine learning models like RF and GBT are often considered "black boxes," hindering the understanding of their decision-making processes. SHAP analysis can address this limitation by quantifying the contribution of each feature to individual predictions, improving model transparency and informing evidence-based decision-making in land cover mapping (Avci et al., 2023; Farda, 2017).

The SVM and naïve Bayes methods perform poorly, making them unsuitable for LULC classification. The SVM has only 36.25% accuracy and 25.33% kappa, with the most extended runtime of 3.868 s, indicating poor predictive ability and high computational cost. Naïve Bayes is even worse, with the lowest accuracy (28.75%) and kappa coefficient (17.12), despite a runtime similar to that of random forest (2.758 s). These results highlight the limitations of these methods in handling the complexities of LULC data, particularly in arid and semi-arid regions. The superior performance of the random forest aligns with studies in China that have reported better results compared to SVM (Avci et al., 2023). Previous research has also shown that increasing the number of training samples can improve the accuracy and efficiency of random forests in land cover classification (Badapalli et al., 2025; Zhao et al., 2024). Class imbalance can bias land cover classification results, leading to issues such as grassland overclassification (GBT) and poor cropland detection (Naïve Bayes) (Almalki et al., 2022). Techniques like SMOTE (generating synthetic samples) and Focal Loss (penalizing rare class misclassification) can mitigate these issues (Hinojosa Lee et al., 2024).

5.3. Performance Metrics on F-1 and Weighted F-1

The F1-scores and weighted average F1-scores provide a more detailed assessment of the algorithms' performance across individual land cover classes. Naïve Bayes exhibits the lowest average F1 score (0.23), reflecting its poor performance in classifying all land cover types. Gradient boosting and CART perform reasonably well, with F1 scores of 0.77 and 0.68, respectively. Gradient Boost excels in cropland (0.69) and built-up areas (0.81), effectively managing nonlinear relationships and minimizing misclassification. The CART shows strong results in dryland forests (0.70) and sparse shrublands (0.70) but struggles with croplands (0.53). Both models balance precision and recall, which is ideal for LULC classification. However, gradient boosting's higher F1 score indicates superior reliability for highly accurate applications, while CART's interpretability remains valuable.

The random forest outperforms all the models, with a weighted average F1 score of 0.85, the highest of the tested algorithms. It accurately classifies cropland (F1 score of 0.82), sparse shrubland (0.89), and built-up areas (0.85), with few misclassification errors. This superior performance stems from its ensemble learning approach, effectively managing the complexity and variability of LULC data. The high F1 scores show a balanced trade-off between precision and recall,

making the random forest model the most reliable model for LULC classification. Its robustness makes it ideal for environmental monitoring and land-use planning applications requiring precise land cover data classification.

5.4. Machine Learning Classifier Parameterization and Performance Limitations

The study employed basic parameterization for the machine learning classifiers, limiting their potential performance. Future research should focus on advanced hyperparameter tuning to optimize the performance of each algorithm. Random Forest utilized 70 trees, and Gradient Boosting Trees employed 100, but other critical parameters like "maxDepth" and "learningRate" were absent. SVM, CART, and Naïve Bayes relied on default settings with no hyperparameter tuning. This lack of optimization contributed to suboptimal results, particularly for SVM (36.25% accuracy) and Naïve Bayes (28.75% accuracy). The absence of fine-tuning, especially concerning "*maxDepth*", "*minLeafPopulation*", "*learningRate*", and kernel configurations, significantly limited these models' robustness and generalization capability.

This study highlights the potential for improved classification accuracy through targeted refinement strategies. Future work should prioritize advanced hyperparameter tuning across all models, including exploring techniques to address class imbalance.

5.5. Study Limitation

The study's limitations include using single-date Landsat-9 imagery (January-April 2023), neglecting seasonal dynamics and potentially misclassifying spectrally similar classes. The lack of hyperparameter tuning and the absence of deep learning methods and advanced techniques for handling class imbalance restricted the comparability with state-of-the-art approaches. The absence of post-classification refinement, including noise filtering and texture analysis, diminished map accuracy. Addressing these gaps with multi-temporal data, hybrid modeling, and advanced hyperparameter tuning while managing class imbalances is crucial for enhancing the robustness of future LULC studies in arid and semi-arid regions.

6. Conclusion

This study rigorously assessed the performance of five distinct machine learning classifiers Random Forest (RF), Gradient Boosted Trees (GBT), Classification and Regression Trees (CART), Support Vector Machine (SVM), and Naïve Bayes for land use and land cover (LULC) classification using Landsat-9 imagery captured between January and April 2023. The objective was to understand the capabilities of these algorithms in the challenging context of arid and semi-arid environments, which present unique complexities for accurate land cover mapping.

The results indicate that Random Forest (RF) excels in this application, demonstrating superior overall accuracy (84.4%), a robust kappa statistic (81.7%), and a

high weighted average F1 score (0.85). This superior performance suggests that RF effectively captures the intricate relationships within the Landsat-9 data and accurately distinguishes between various land cover types. Gradient Boosting Trees (GBT) emerged as a viable alternative, exhibiting competitive performance (76.9% accuracy, 0.77 F1 score), and demonstrating strength in classifying cropland and built-up areas. While CART yielded lower accuracy, its inherent interpretability offers a valuable advantage in scenarios where understanding the decision-making process is paramount. In contrast, Naïve Bayes and SVM significantly underperformed, achieving accuracy below 40% and F1 scores below 0.30. This highlights the limitations of these models in handling the complexities of LULC classification, potentially stemming from simplifying assumptions, model inflexibility, and suboptimal hyperparameter tuning.

Furthermore, the study revealed common challenges across all models, including the impact of class imbalance, a tendency to overclassify dominant land cover types, and the recognized need for more sophisticated parameter optimization strategies. While this research provides valuable insights, it's essential to acknowledge its limitations. The reliance on single-date imagery, the exclusion of deep learning models, the constraints on parameter tuning, and the absence of post-classification refinement techniques likely limited the full potential of the evaluated classifiers.

Future research should address these limitations to further enhance the accuracy, robustness, and generalizability of LULC classification models. Potentially, this would incorporate multi-temporal datasets, explore advanced deep learning architectures, employ more extensive hyperparameter optimization techniques, and implement post-classification refinement procedures. Ultimately, continued advancements in these areas will contribute significantly to improved land resource management, environmental monitoring, and sustainable development practices in arid and semi-arid regions.

7. Recommendation

To enhance land use and land cover (LULC) classification accuracy, prioritize the Random Forest algorithm for its robust performance in classifying complex land cover. Gradient Boosted Trees and Classification and Regression Trees serve as viable alternatives, each offering distinct advantages in terms of accuracy and interpretability, respectively. Minimize the use of Support Vector Machine and Naïve Bayes in similar studies, particularly with complex datasets without substantial optimization. Future research should investigate hybrid models and tackle class imbalance using techniques like SMOTE or Focal Loss. Leverage multi-temporal imagery to capture seasonal changes and employ post-classification refinement methods such as noise filtering and texture analysis to improve map quality.

Author Contributions

John Kapoi Kipterer: writing-original draft, investigation, visualisation, conceptualisation, data collection and analysis, remote sensing data analysis and compi-

lation. **Mark Boitt:** Methodology review, editing, and alignment of the content. **Charles, N Mundia:** Writing-review, methodology review and remote sensing image alignment and validation.

Data Availability

The data presented in this manuscript and the Java and R scripts used are comprehensive and openly available for further research and access upon request.

Conflicts of Interest

The authors declare no conflicts of interest regarding the publication of this paper.

References

Abebe, G., Getachew, D., & Ewunetu, A. (2022). Analysing Land Use/Land Cover Changes and Its Dynamics Using Remote Sensing and GIS in Gubalafito District, Northeastern Ethiopia. *SN Applied Sciences, 4,* Article No. 30. https://doi.org/10.1007/s42452-021-04915-8

Adugna, T., Xu, W., & Fan, J. (2022). Comparison of Random Forest and Support Vector Machine Classifiers for Regional Land Cover Mapping Using Coarse Resolution FY-3C Images. *Remote Sensing, 14,* Article 574. https://doi.org/10.3390/rs14030574

Almalki, R., Khaki, M., Saco, P. M., & Rodriguez, J. F. (2022). Monitoring and Mapping Vegetation Cover Changes in Arid and Semi-Arid Areas Using Remote Sensing Technology: A Review. *Remote Sensing, 14,* Article 5143. https://doi.org/10.3390/rs14205143

Amani, M., Ghorbanian, A., Ahmadi, S. A., Kakooei, M., Moghimi, A., Mirmazloumi, S. M., et al. (2020). Google Earth Engine Cloud Computing Platform for Remote Sensing Big Data Applications: A Comprehensive Review. *IEEE Journal of Selected Topics in Applied Earth Observations and Remote Sensing, 13,* 5326-5350. https://doi.org/10.1109/jstars.2020.3021052

Amboka, A. A., & Ngigi, T. G. (2015). Mapping and Monitoring Spatial-Temporal Cover Change of Prosopis Species Colonization in Baringo Central, Kenya. *International Journal of Engineering Science Invention, 4,* 50-55. https://www.ijesi.org/papers/Vol(4)3/Version-1/I0431050057.pdf

Amwata, D. A., & Nyariki, D. M. (2021). Climate Variability, Land-Use, Pastoral and Agropastoral Livelihoods in Arid and Semi-Arid Areas of Kenya. *World Journal of Innovative Research, 10,* 117-126. https://doi.org/10.31871/wjir.10.5.38

Avci, C., Budak, M., Yağmur, N., & Balçik, F. (2023). Comparison between Random Forest and Support Vector Machine Algorithms for LULC Classification. *International Journal of Engineering and Geosciences, 8,* 1-10. https://doi.org/10.26833/ijeg.987605

Badapalli, P. K., Nakkala, A. B., Gugulothu, S., & Kottala, R. B. (2025). Dynamic Land Degradation Assessment: Integrating Machine Learning with Landsat 8 OLI/TIRS for Enhanced Spectral, Terrain, and Land Cover Indices. *Earth Systems and Environment, 9,* 315-335. https://doi.org/10.1007/s41748-024-00442-9

Bogale, G. A., Mosisa, T., & Asefa, G. (2022). The Impacts of Land Use/Land Cover Change on Range Land Biodiversity in Ethiopia: Review. *Journal of Biodiversity & Endangered Species, 10,* 1-6.

Bollig, M., & Österle, M. (2013). The Political Ecology of Specialisation and Diversification: Long-Term Dynamics of Pastoralism in East Pokot District, Kenya. In M. Bollig, M. Schnegg, & H.-P. Wotzka (Eds.), *Pastoralism in Africa: Past, Present, and Futures* (pp.

289-315). Berghahn Books. https://www.researchgate.net/publication/285526843

Bollig, M., Greiner, C., & Österle, M. (2014). Inscribing Identity and Agency on the Landscape: Of Pathways, Places, and the Transition of the Public Sphere in East Pokot, Kenya. *African Studies Review, 57,* 55-78. https://doi.org/10.1017/asr.2014.92

Cao, Z., Wang, S., Luo, P., Xie, D., & Zhu, W. (2022). Watershed Ecohydrological Processes in a Changing Environment: Opportunities and Challenges. *Water, 14,* Article 1502. https://doi.org/10.3390/w14091502

Chen, W., Shirzadi, A., Shahabi, H., Ahmad, B. B., Zhang, S., Hong, H., et al. (2017). A Novel Hybrid Artificial Intelligence Approach Based on the Rotation Forest Ensemble and Naïve Bayes Tree Classifiers for a Landslide Susceptibility Assessment in Langao County, China. *Geomatics, Natural Hazards and Risk, 8,* 1955-1977. https://doi.org/10.1080/19475705.2017.1401560

Chowdhury, M. S. (2024). Comparison of Accuracy and Reliability of Random Forest, Support Vector Machine, Artificial Neural Network and Maximum Likelihood Method in Land Use/Cover Classification of Urban Setting. *Environmental Challenges, 14,* Article 100800. https://doi.org/10.1016/j.envc.2023.100800

Earth Resources Observation and Science (EROS) Center. (2020). *Landsat 8-9 Operational Land Imager/Thermal Infrared Sensor Level-2, Collection 2*. U.S. Geological Survey.

Elmahdy, S. I., & Mohamed, M. M. (2023). Regional Mapping and Monitoring Land Use/Land Cover Changes: A Modified Approach Using an Ensemble Machine Learning and Multitemporal Landsat Data. *Geocarto International, 38,* Article 2184500. https://doi.org/10.1080/10106049.2023.2184500

Fang, Z., Ding, T., Chen, J., Xue, S., Zhou, Q., Wang, Y., et al. (2022). Impacts of Land Use/Land Cover Changes on Ecosystem Services in Ecologically Fragile Regions. *Science of The Total Environment, 831,* Article 154967. https://doi.org/10.1016/j.scitotenv.2022.154967

Farda, N. M. (2017). Multi-Temporal Land Use Mapping of Coastal Wetlands Area Using Machine Learning in Google Earth Engine. *IOP Conference Series: Earth and Environmental Science, 98,* Article 012042. https://doi.org/10.1088/1755-1315/98/1/012042

Fentaw, A. E., & Abegaz, A. (2024). Analyzing Land Use/Land Cover Changes Using Google Earth Engine and Random Forest Algorithm and Their Implications to the Management of Land Degradation in the Upper Tekeze Basin, Ethiopia. *The Scientific World Journal, 2024,* Article ID: 3937558. https://doi.org/10.1155/2024/3937558

Firthouse Mohammed Yashin, J., Deivanayagam, A., Rahaman Sheik Mohideen, A., & Rajagopal, J. (2020). Comparative Analysis of Classification Algorithms for Landuse/Landcover Change over a Part of the East Coast Region of Tamil Nadu and Its Environs. In Institute of Electrical and Electronics Engineers (Ed.), *2020 IEEE India Geoscience and Remote Sensing Symposium (InGARSS)* (pp. 66-69). IEEE. https://doi.org/10.1109/ingarss48198.2020.9358945

Ghosh, S., Kumar, D., & Kumari, R. (2022). Cloud-Based Large-Scale Data Retrieval, Mapping, and Analysis for Land Monitoring Applications with Google Earth Engine (GEE). *Environmental Challenges, 9,* Article 100605. https://doi.org/10.1016/j.envc.2022.100605

Greiner, C., Greven, D., & Klagge, B. (2021a). Roads to Change: Livelihoods, Land Disputes, and Anticipation of Future Developments in Rural Kenya. *The European Journal of Development Research, 33,* 1044-1068. https://doi.org/10.1057/s41287-021-00396-y

Greiner, C., Vehrs, H., & Bollig, M. (2021b). Land-Use and Land-Cover Changes in Pastoral Drylands: Long-Term Dynamics, Economic Change, and Shifting Socioecological Frontiers in Baringo, Kenya. *Human Ecology, 49,* 565-577.

https://doi.org/10.1007/s10745-021-00263-8

Hinojosa Lee, M. C., Braet, J., & Springael, J. (2024). Performance Metrics for Multilabel Emotion Classification: Comparing Micro, Macro, and Weighted F1-Scores. *Applied Sciences, 14,* Article 9863. https://doi.org/10.3390/app14219863

Kapoi, K. J., & Charles, N. M. (2015). Livelihood Vulnerability Assessment in the Context of Drought Hazard: A Case Study of Baringo County, Kenya. *International Journal of Science and Research, 3,* 346-349.

Kiage, L. M., & Douglas, P. (2020). Linkages between Land Cover Change, Lake Shrinkage, and Sublacustrine Influence Determined from Remote Sensing of Select Rift Valley Lakes in Kenya. *Science of The Total Environment, 709,* Article 136022. https://doi.org/10.1016/j.scitotenv.2019.136022

Kimtai, D. J., Makokha, G. O., & Sichangi, A. W. (2024). Modeling of Water Level Trends and Characterizing Potential Influencing Factors in Lake Baringo in Kenya. *Discover Water, 4,* Article No. 55. https://doi.org/10.1007/s43832-024-00105-w

Kumar Basukala, A., Vehrs, H.-P., Bollig, M., Greiner, C., & Thonfeld, F. (2019). *Dataset: Spatial-Temporal Analysis of Land-Use and Land-Cover Change in East Pokot, Kenya.* https://www.researchgate.net/profile/Amit-Basukala/publication/338858573_Dataset_Spatial-temporal_analysis_of_land-use_and_land-cover_change_in_East_Pokot_Kenya/links/661e560443f8df018d129c29/Dataset-Spatial-temporal-analysis-of-land-use-and-land-cover-change-in-East-Pokot-Kenya.pdf

Li, S., Xu, L., Jing, Y., Yin, H., Li, X., & Guan, X. (2021). High-Quality Vegetation Index Product Generation: A Review of NDVI Time Series Reconstruction Techniques. *International Journal of Applied Earth Observation and Geoinformation, 105,* Article 102640. https://doi.org/10.1016/j.jag.2021.102640

Lipton, Z. C., Elkan, C., & Naryanaswamy, B. (2014). Optimal Thresholding of Classifiers to Maximize F1 Measure. In T. Calders, F. Esposito, E. Hüllermeier, & R. Meo (Eds.), *Machine Learning and Knowledge Discovery in Databases ECML PKDD 2014* (pp. 225-239). Springer. https://doi.org/10.1007/978-3-662-44851-9_15

Maini, S. S., & Govinda, K. (2017). Stock Market Prediction Using Data Mining Techniques. In Institute of Electrical and Electronics Engineers (Ed.), *2017 International Conference on Intelligent Sustainable Systems (ICISS)* (pp. 654-661). IEEE. https://doi.org/10.1109/iss1.2017.8389253

Mayer, T., Poortinga, A., Bhandari, B., Nicolau, A. P., Markert, K., Thwal, N. S., et al. (2021). Deep Learning Approach for Sentinel-1 Surface Water Mapping Leveraging Google Earth Engine. *ISPRS Open Journal of Photogrammetry and Remote Sensing, 2,* Article 100005. https://doi.org/10.1016/j.ophoto.2021.100005

Mbaabu, P. R., Ng, W., Schaffner, U., Gichaba, M., Olago, D., Choge, S., et al. (2019). Spatial Evolution of Prosopis Invasion and Its Effects on LULC and Livelihoods in Baringo, Kenya. *Remote Sensing, 11,* Article 1217. https://doi.org/10.3390/rs11101217

Ochuka, M., Ikporukpo, C., Mijinyawa, Y., & Ogendi, G. (2019). Land Use/Land Cover Dynamics and Anthropogenic Driving Factors in Lake Baringo Catchment, Rift Valley, Kenya. *Natural Resources, 10,* 367-389. https://doi.org/10.4236/nr.2019.1010025

Pham, H., Nguyen, H., Le, K., Tran, T., & Ha, N. (2023). Automated Mapping of Wetland Ecosystems: A Study Using Google Earth Engine and Machine Learning for Lotus Mapping in Central Vietnam. *Water, 15,* Article 854. https://doi.org/10.3390/w15050854

Praticò, S., Solano, F., Di Fazio, S., & Modica, G. (2021). Machine Learning Classification of Mediterranean Forest Habitats in Google Earth Engine Based on Seasonal Sentinel-2 Time-Series and Input Image Composition Optimisation. *Remote Sensing, 13,* Article 586. https://doi.org/10.3390/rs13040586

Rikimaru, A., Roy, P.S., & Miyatake, S. (2002). Tropical Forest Cover Density Mapping. *International Society for Tropical Ecology, 43,* 39-47.

Sun, J., & Ongsomwang, S. (2023). Optimal Parameters of Random Forest for Land Cover Classification with Suitable Data Type and Dataset on Google Earth Engine. *Frontiers in Earth Science, 11,* Article 1188093. https://doi.org/10.3389/feart.2023.1188093

Talukdar, S., Singha, P., Mahato, S., Shahfahad, Pal, S., Liou, Y., et al. (2020). Land-Use Land-Cover Classification by Machine Learning Classifiers for Satellite Observations—A Review. *Remote Sensing, 12,* Article 1135. https://doi.org/10.3390/rs12071135

Tamayo-Vera, D., Wang, X., & Mesbah, M. (2024). A Review of Machine Learning Techniques in Agroclimatic Studies. *Agriculture, 14,* Article 481. https://doi.org/10.3390/agriculture14030481

Vehrs, H. (2016). Changes in Landscape Vegetation, Forage Plant Composition and Herding Structure in the Pastoralist Livelihoods of East Pokot, Kenya. *Journal of Eastern African Studies, 10,* 88-110. https://doi.org/10.1080/17531055.2015.1134401

Wang, J., Bretz, M., Dewan, M. A. A., & Delavar, M. A. (2022). Machine Learning in Modelling Land-Use and Land Cover-Change (LULCC): Current Status, Challenges and Prospects. *Science of The Total Environment, 822,* Article 153559. https://doi.org/10.1016/j.scitotenv.2022.153559

Zha, Y., Gao, J., & Ni, S. (2003). Use of Normalized Difference Built-Up Index in Automatically Mapping Urban Areas from TM Imagery. *International Journal of Remote Sensing, 24,* 583-594. https://doi.org/10.1080/01431160304987

Zhao, Z., Islam, F., Waseem, L. A., Tariq, A., Nawaz, M., Islam, I. U., et al. (2024). Comparison of Three Machine Learning Algorithms Using Google Earth Engine for Land Use Land Cover Classification. *Rangeland Ecology & Management, 92,* 129-137. https://doi.org/10.1016/j.rama.2023.10.007